



# Utility of contrast-enhanced ultrasound in differential diagnosis of adrenal tumors in dogs

Takahiro NAGUMO<sup>1)</sup>, Kumiko ISHIGAKI<sup>1)</sup>, Oriie YOSHIDA<sup>1)</sup>, Keigo IIZUKA<sup>1)</sup>, Kei TAMURA<sup>1)</sup>, Naoki SAKURAI<sup>1)</sup>, Kazuyuki TERAJ<sup>1)</sup>, Mamiko SEKI<sup>1)</sup>, Kazuya EDAMURA<sup>1)</sup> and Kazushi ASANO<sup>1)\*</sup>

<sup>1)</sup>Laboratory of Veterinary Surgery, Department of Veterinary Medicine, College of Bioresource Sciences, Nihon University, 1886 Kameino, Fujisawa, Kanagawa 252-0880, Japan

**ABSTRACT.** This prospective case study aimed to clarify the clinical significance of contrast-enhanced ultrasound (CEUS) for the differential diagnosis of canine adrenal tumors. Forty-three client-owned dogs with adrenal tumors were included. All dogs underwent CEUS, which was evaluated qualitatively and quantitatively. The peak signal intensity (PI), time to peak signal intensity (TPI), mean transit time (MTT), upslope, and downslope were calculated for each time-intensity curve. The histopathological diagnosis of each resected mass was compared with the CEUS findings and parameters. Enhancement distribution, vascularity, tortuous nourishing vessels, enhancement pattern, and late-phase enhancement did not differ significantly between adrenal cortical adenoma (CA), adenocarcinoma (CAC), and pheochromocytoma (PHEO) in qualitative assessment. In PHEO, the TPI was significantly more rapid compared with that in CA ( $P=0.0287$ ) and CAC ( $P=0.0404$ ). The MTT in PHEO was significantly shorter than that in CA ( $P=0.0016$ ) and CAC ( $P=0.0003$ ). Upslope in PHEO was larger than that in CAC ( $P=0.0406$ ). Downslope in PHEO was significantly larger than that in CA ( $P=0.0048$ ) and CAC ( $P=0.0018$ ). A receiver operating characteristic curve analysis demonstrated that the area under the MTT curve yielded 0.91 for distinguishing PHEO from adrenocortical tumors in dogs; an MTT cut-off value less than 6,225 msec yielded a sensitivity of 69%, specificity of 94%, and likelihood ratio of 12.46. CEUS appears to be clinically applicable for the differential diagnosis between cortical and medullary origins of primary adrenal tumors in dogs.

**KEY WORDS:** adrenal tumor, contrast-enhanced ultrasound, dog, sonazoid

*J. Vet. Med. Sci.*

82(11): 1594–1601, 2020

doi: 10.1292/jvms.20-0427

Received: 15 July 2020

Accepted: 13 September 2020

Advanced Epub:

24 September 2020

In dogs, primary adrenal gland tumors account for approximately 0.17 to 0.76% of all neoplasias [17]. The most common adrenal tumors in dogs include cortical adenoma (CA), cortical adenocarcinoma (CAC), and pheochromocytoma (PHEO). Adrenalectomy is the treatment of choice for adrenal masses [1, 4, 15, 16, 18, 27, 30]. In dogs with adrenal tumors, the risk factors for mortality include the type of primary adrenal gland tumor [3], whereas treatment with an  $\alpha$ -adrenergic antagonist (e.g., phenoxybenzamine) before the removal of a PHEO is reported to result in a significant decrease in the mortality rate [14]. In case of functional adrenocortical tumors, preoperative administration of trilostane reduces the perioperative complications associated with Cushing's syndrome [5].

The measurement of urinary and plasma catecholamines and metanephrines is useful for the preoperative differential diagnosis of PHEO [11, 26]. However, not all cases of PHEO present with high levels of urinary and plasma catecholamines and metanephrines. Therefore, these measurements are not sufficient to distinguish between the cortical or medullary origin in a case involving a nonfunctional adrenal tumor.

Ultrasonographic examination is reported to yield a sensitivity of 63.7% and specificity of 100% for the identification of adrenal lesions [22]. Moreover, ultrasonographic identification of a tumor thrombus in the caudal vena cava (CVC) by adrenal tumors has a sensitivity of 100% and specificity of 96% [7]. Adrenal gland lesions (more than 20 mm in diameter) and vascular invasion are considered criteria for predicting malignant neoplasms [22]. However, these parameters are not useful in the differential diagnosis of adrenal tumors in dogs. A previous retrospective study demonstrated that ultrasound-guided fine-needle aspiration (FNA) can accurately distinguish adrenal cortical tumors from PHEO in dogs, with accuracy rates of 90 to 100% [6]. However, some adrenocortical carcinomas exhibit a relatively benign cellular morphology [31]. Additionally, a previous study reported

\*Correspondence to: Asano, K.: asano.kazushi@nihon-u.ac.jp

©2020 The Japanese Society of Veterinary Science



This is an open-access article distributed under the terms of the Creative Commons Attribution Non-Commercial No Derivatives (by-nc-nd) License. (CC-BY-NC-ND 4.0: <https://creativecommons.org/licenses/by-nc-nd/4.0/>)

that FNA for PHEO might cause ventricular tachycardia [28]. It also increases the potential risk of hemorrhage due to abundant blood inflow in the lesion. We have previously demonstrated that triple-phase helical computed tomography (CT) has the potential for preoperative differential diagnosis of adrenal tumors in dogs [32]; however, the procedure requires general anesthesia, and in dogs with PHEO, hypertension and tachycardia might occur during general anesthesia. Therefore, less invasive and more simple techniques are desirable for the differential diagnosis of adrenal tumors in dogs.

In humans, contrast-enhanced ultrasound (CEUS) is applied in the differential diagnosis of liver tumors and other pathological conditions [12, 13]. In small animal medicine, CEUS is reported to have a diagnostic accuracy level exceeding 95% for distinguishing benign from malignant tumors in the liver [21]. Recent studies have reported the utility of CEUS in the diagnosis of lesions in the spleen and pancreas in dogs [20, 29]. However, only a limited number of reports have described the usefulness of CEUS in the diagnosis of normal canine adrenal gland, pituitary-dependent hyperadrenocorticism, and adrenal tumors [2, 23–25]. In a previous study on CEUS for the diagnosis of adrenal tumors, the combination of enhancement degree and vascularity demonstrated to differentiate among CA, CAC and PHEO with an accuracy of 91.7% [2]. We hypothesized that CEUS is a convenient and promising technique for the differential diagnosis of canine adrenal tumors. Therefore, this study aimed to determine the feasibility of CEUS using sonazoid for the differential diagnosis of canine adrenal tumors.

## MATERIALS AND METHODS

### Study design

This study was a prospective case study. All dogs were referred to our hospital with a suspicion of primary adrenal masses between February 2016 and September 2018. Informed owner consent was obtained prior to inclusion of the dogs in the study. The dogs were evaluated by physical examinations, blood and urine tests, radiography, and ultrasonography in our hospital.

The inclusion criteria of this study were dogs with adrenal masses showing the contrast enhancement by CEUS. After the CEUS, adrenalectomy was performed in all dogs. All resected tumors were performed in histopathological diagnosis.

### CEUS

All dogs underwent CEUS as follows: a suspension of perflubutane (sonazoid, Daiichi-Sankyo Corp., Tokyo, Japan) was prepared with 2 ml of saline at an 8- $\mu$ l/ml concentration. An ultrasound machine (Aplio400, Canon Medical Systems Corp., Tochigi, Japan) was used with a 6-MHz convex probe for CEUS on the day before the operation or on the day of the operation. In all dogs, a 22- or 24-gauge intravenous catheter was inserted in the cephalic vein depending on the animal's size. Sonazoid was injected intravenously at a volume of 0.015 ml/kg (0.12  $\mu$ l/kg perflubutane), followed by a 5-ml saline injection. A sagittal view of the adrenal mass under contrast harmonic imaging (CHI) mode was recorded for 2 min after the saline flush. The ultrasonographic examination was withdrawn, followed by another recording from 4.5 to 5 min after the saline injection. Mechanical index was set under 0.2, and ultrasonography was performed by a veterinarian. The dogs were not sedated or anesthetized.

### CEUS image analysis

All images were analyzed by a veterinarian. The images were qualitatively evaluated as follows: (1) enhancement distribution (homogeneous or heterogeneous pattern); (2) vascularity (enhancement of the visible nourishing vessels in the mass at the arterial phase); (3) tortuous nourishing vessels; (4) enhancement pattern (directivity of enhancement, categorized as centripetal, centrifugal, disordered, or nodular pattern at the arterial phase); and (5) late-phase enhancement (enhancement at 5 min after injection of perflubutane). Vascularity was defined as a line-like enhancement indicating the visible nourishing vessels before the enhancement of whole mass. In cases with vascularity, when the line-like enhancement showed a curve, it was defined as tortuous nourishing vessels (Fig. 1). In the enhancement pattern, centripetal was defined as the enhancement from the margin to the center in the mass. Centrifugal was defined as enhancement from the center to the margin in the mass. Disordered was defined as irregular enhancement in the mass. Nodular was defined as the partial enhancement in the mass. The region of interest (ROI) with a diameter of 8 mm was placed on the adrenal mass without including the vessel and non-enhanced region, and a time intensity curve (TIC) was generated. The ROI position was corrected to allow minimum body movement and respiration (ROI tracking).

An approximate curve was generated from the TIC by the available software (GraphPad Prism, version 6.0 for Macintosh, Graph Pad Software Inc., San Diego, CA, USA). Peak signal intensity (PI), time to peak signal intensity (TPI), mean transit time (MTT), upslope, and downslope were calculated for each tumor. PI was defined as the value corresponding to the highest intensity. TPI was defined as the interval between the initial rise and attainment of its maximum signal intensity. MTT was defined as the interval between the arrival at 50% PI and the attainment of a 50% decrease in PI. The upslope was defined as the slope of 10–85% PI, and was calculated in  $(85\% \text{ PI} - 10\% \text{ PI}) / (\text{Time at } 85\% \text{ PI} - \text{Time at } 10\% \text{ PI})$ . The downslope was defined as the slope of 85–40% PI, and was calculated in  $(85\% \text{ PI} - 40\% \text{ PI}) / (\text{Time at } 40\% \text{ PI} - \text{Time at } 85\% \text{ PI})$  (Fig. 2).

### Statistical analysis

Statistical tests were performed using the commercially available statistical analysis software (GraphPad Prism, version 6.0 for Macintosh). The qualitative evaluation parameters, including the enhancement distribution, vascularity, enhanced vessel tortuosity, enhancement pattern, and late-phase enhancement, were analyzed using the  $\chi^2$  test. The PI, TPI, MTT, upslope, and downslope were statistically compared between CA, CAC, and PHEO using Kruskal-Wallis test followed by Dunn's post hoc correction test. Differences in the values were considered statistically significant at  $P < 0.05$ . For parameters that had significant differences among

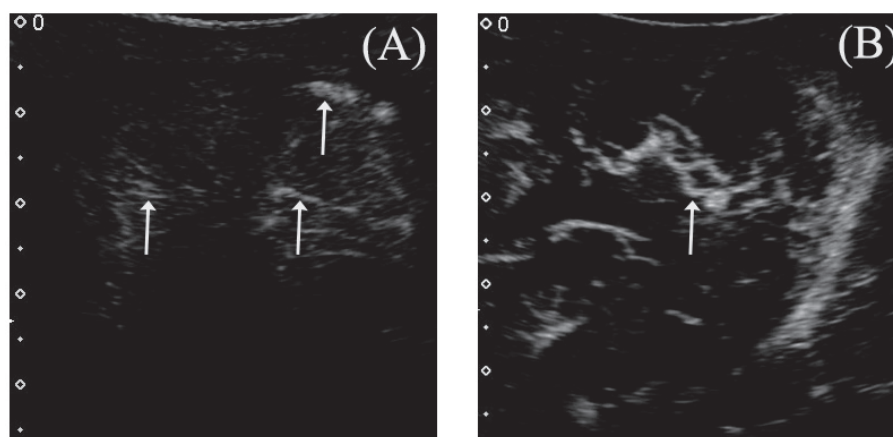


**Fig. 1.** Typical image of vascularity in qualitative assessment. (A) A line-like enhancement of arteriole (white arrows) in the mass at the arterial phase. (B) A tortuosity of arteriole (white arrow) in the mass at the arterial phase.

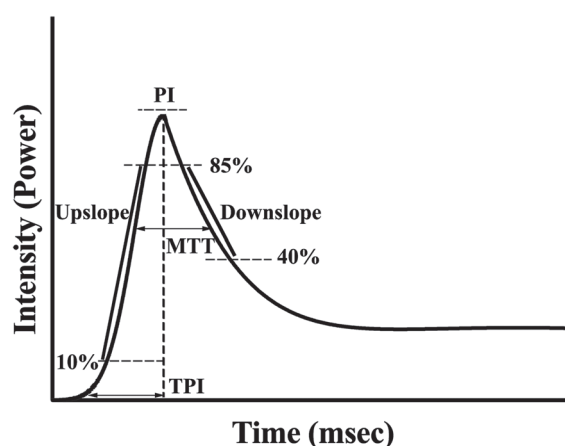


**Fig. 2.** Schematic illustration of each parameter measured from the time intensity curve (TIC). PI, peak signal intensity, the value corresponding to the highest intensity; TPI, time to peak signal intensity, the interval between the initial rise and attainment of its maximum signal intensity; MTT, mean transit time, the interval between the arrival at 50% PI and the attainment of a 50% decrease in PI; Upslope, the slope of 10–85% PI; Downslope, the slope of 85–40% PI.

both CAs and PHEOs, CACs and PHEOs, we generated receiver operating characteristic (ROC) curves, the areas under the curve (AUC) and determined the cut-off values, sensitivity, specificity, positive likelihood and negative likelihood. In addition, 95% confidence intervals (CIs) in AUC, sensitivity and specificity were calculated.

## RESULTS

### Case information

Forty-three client-owned dogs met the inclusion criteria and were enrolled in this study. Three dogs did not meet the inclusion criteria and were excluded in this study. The median age of dogs included in this study was 11.8 years (range, 6.0–14.6 years). The 43 dogs included 19 males (14 neutered) and 24 females (23 spayed). The median bodyweight of the dogs was 5.7 kg (range, 2.3–26.0 kg). Breeds were as follows: 10 Miniature Dachshunds; 7 Chihuahuas; 6 Shih Tzus, 5 Toy Poodles; 3 Miniature Schnauzers; Cavalier King Charles Spaniels and Pomeranians, and Mixed breeds, 2 each; and West Highland White Terrier, Welsh Corgi, Shiba, Bulldog, Yorkshire Terrier, and Labrador Retriever, 1 each.

A total of 44 resected masses were obtained from 43 dogs (1 with bilateral adrenal tumors). The diagnoses included CA (6 masses), CAC (12 masses), and PHEO (26 masses). The tumor location was on the right side in 26/44 masses (59%) and on the left side in 18/44 masses (41%). Of the 44 masses, 21 (CAC, 3; PHEO, 18) had exhibited the gross findings of tumor thrombus formation into the CVC. The histopathological examination revealed vascular invasion in 28 masses (CAC, 5; PHEO, 23). Of the 44 masses, 5 (CAC, 2; PHEO, 3) and 3 (CA, 1; CAC, 1; PHEO, 1) contained intratumoral necrosis and hemorrhage, respectively.

Of the 17 cases involving adrenal cortical tumors, 10 (CA, 3; CAC, 7) showed the clinical signs of Cushing's syndrome

(polyuria/polydipsia, abdominal distention, and alopecia). Of the 26 cases with PHEO, 17 had tachycardia (more than 160 bpm), hypertension (systolic blood pressure more than 160 mmHg or diastolic blood pressure more than 100 mmHg), and ventricular arrhythmia at the first consultation or during the operation. The median systolic, diastolic, and mean arterial pressures measured using the oscillometric method were 148 mmHg (range, 109–192 mmHg), 98 mmHg (range, 50–176 mmHg), and 114 mmHg (range, 72–180 mmHg), respectively.

### Qualitative assessment

The qualitative assessment is summarized in Table 1. Of the 44 masses, 2 were excluded from the qualitative analysis due to an inadequate image quality. The enhancement distribution did not differ significantly among the tumor types ( $P=0.2120$ ). The tumor types did not differ significantly with respect to vascularity ( $P=0.2954$ ). The tumor types did not differ with respect to tortuosity ( $P=0.1861$ ). The enhancement pattern did not differ significantly among the tumor types ( $P=0.4408$ ). Although CA tended to exhibit an increase in late-phase enhancement, there was no significant difference among the tumor types ( $P=0.2449$ ). PHEO was characterized by a rapid increase and decrease in enhancement, whereas CA and CAC were characterized by a delayed decrease in enhancement (Fig. 3).

### Quantitative assessment

The quantitative assessment is summarized in Table 2. TIC was derived from all 44 masses. A typical TIC corresponding to each tumor type is shown in Fig. 4. Although the PI tended to be higher in PHEOs than other types, it did not differ significantly among the 3 tumor types ( $P=0.0895$ ). In PHEO, TPI was significantly more rapid than that in CA ( $P=0.0287$ ) and CAC ( $P=0.0404$ ). In addition, MTT in PHEO was also significantly shorter than that in CA ( $P=0.0016$ ) and CAC ( $P=0.0003$ ). Upslope in PHEO was also larger than that in CAC ( $P=0.0406$ ). In contrast, downslope in PHEO was significantly larger than that in CA ( $P=0.0048$ ) and CAC ( $P=0.0018$ ). According to the ROC analysis (Fig. 5), AUCs were 0.78 for TPI (95% CI: 0.64–0.92,  $P=0.001628$ ), 0.91 for MTT (95% CI: 0.83–0.99,  $P<0.0001$ ), and 0.87 for the downslope (95% CI: 0.77–0.97,  $P<0.0001$ ). To distinguish PHEO from adrenocortical tumors in dogs, a TPI cut-off value of less than 3,444 msec provided a sensitivity of 38% (95% CI: 20–59%), specificity of 94% (95% CI: 73–100%), positive likelihood ratio of 6.923 and negative likelihood ratio of 0.651. An MTT cut-off value of less than 6,225 msec provided a sensitivity of 69% (95% CI: 48–86%), specificity of 94% (95% CI: 73–100%), positive likelihood ratio of 12.46 and negative likelihood ratio of 0.326. A downslope cut-off value of more than  $8.38 \times 10^{-9}$  showed a sensitivity of 58% (95% CI: 33–73%), specificity of 94% (95% CI: 73–100%), positive likelihood ratio of 10.38 and negative likelihood ratio of 0.448.

## DISCUSSION

Our study demonstrated that CEUS has a potential utility for differentiating PHEO from adrenocortical tumors in dogs; however, the characteristic enhancement patterns in both CA and CAC were found to be almost similar. Differential diagnosis between adrenocortical and adrenomedullary tumors might have a great impact on the perioperative medical management associated with surgical outcomes.

In a previous study, a significant difference in the MTT was reported between CA and CAC and between CA and PHEO [24]. However, the study had a small sample size, and the ROI was fitted to the whole tumor, including the enhanced vessels and non-enhanced tissues. Different ROI settings affect the TIC and might account for the different results between the previous and present studies. In our study, 2 parameters (upslope and downslope) were added to the quantitative analysis of CEUS for the evaluation of wash-in and wash-out in the adrenal tumors, and this was not done in a previous study [24]. We observed a significant difference in

**Table 1.** Qualitative assessment of contrast-enhanced ultrasound in canine adrenal tumors

Parameters		CA (n=5)	CAC (n=11)	PHEO (n=26)	P-value
Enhancement distribution	Homogeneous	2	1	3	0.2120
	Heterogeneous	3	10	23	
Vascularity	Presence	3	10	18	0.2954
	Absence	2	1	8	
Tortuosity	Presence	0	4	10	0.1861
	Absence	3	6	8	
Enhancement pattern	Centripetal	1	4	14	0.4408
	Centrifugal	1	2	1	
	Disordered	0	2	8	
	Nodular	3	3	3	
Late-phase enhancement	Presence	3	3	6	0.2449
	Absence	2	8	20	

CA, cortical adenoma; CAC, cortical adenocarcinoma; PHEO, pheochromocytoma.

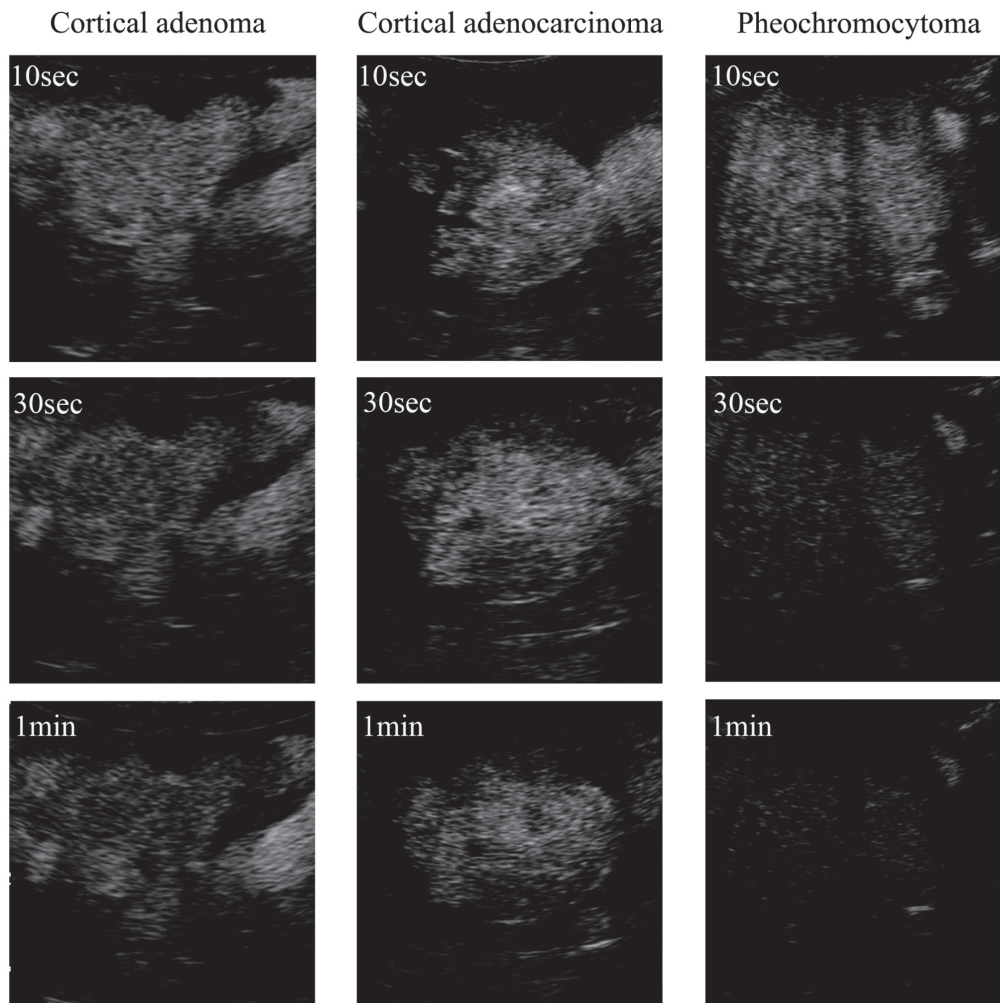


**Fig. 3.** Enhanced images of adrenal cortical adenoma (CA), adrenal cortical adenocarcinoma (CAC), and pheochromocytoma (PHEO) at 10 sec, 30 sec, and 1 min. At 10 sec, CA and CAC are not satisfactorily enhanced; however, desired enhancement is observed in PHEO. At 30 sec, desired enhancement in CA and CAC is observed. The enhanced image of PHEO shows a decrease in signal intensity, and the enhancement starts to decrease. At 1 min, the enhancement starts to decrease in CA and CAC. A larger decrease in enhancement is observed in PHEO at 1 min than that at 30 sec.

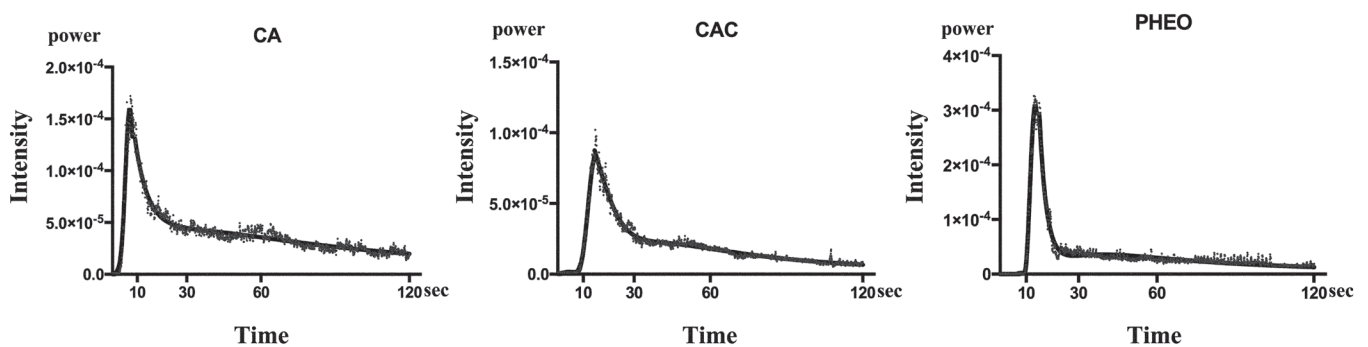


**Fig. 4.** Typical time intensity curve (TIC) of each tumor type. The TIC indicates that pheochromocytoma (PHEO) had a short mean transit time (MTT) and a large downslope and upslope when compared with adrenal cortical adenoma (CA) and adrenal cortical adenocarcinoma (CAC)

the upslope between PHEO and CAC, and significant differences in the downslope of PHEO relative to those of CA and CAC. Our study has objectively demonstrated that the CEUS characteristics of PHEO include a rapid wash-in and wash-out.

In a previous study on the enhancement patterns of adrenal tumors [2], most cases of CA showed a centripetal pattern while most CAC and PHEO lesions had a disordered pattern. However, our study demonstrated that most CAs exhibited a nodular

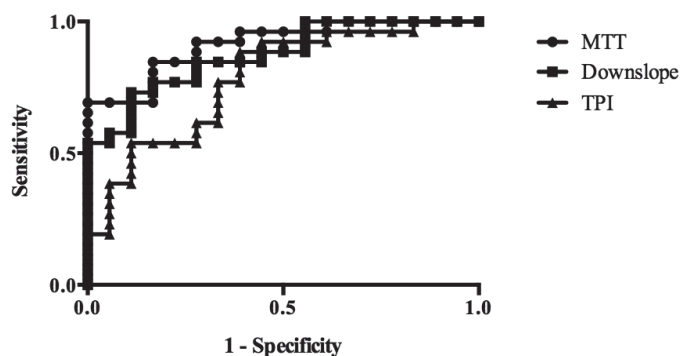


**Fig. 5.** Receiver operating characteristic (ROC) curves in time to peak signal intensity (TPI), mean transit time (MTT) and downslope. ROC curves in TPI, MTT and downslope indicate sensitivity and specificity to identify the origins of primary canine adrenal tumor.

**Table 2.** Quantitative parameters of contrast-enhanced ultrasound in canine adrenal tumors

	CA (n=6)	CAC (n=12)	PHEO (n=26)	P-value		
				CA vs. CAC	CA vs. PHEO	CAC vs. PHEO
PI (power)	$0.59 \times 10^{-4}$ [5.77 × 10 <sup>-6</sup> –1.51 × 10 <sup>-4</sup> ]	$0.74 \times 10^{-4}$ [3.49 × 10 <sup>-6</sup> –4.41 × 10 <sup>-4</sup> ]	$1.05 \times 10^{-4}$ [8.12 × 10 <sup>-6</sup> –2.21 × 10 <sup>-3</sup> ]	>0.9999	0.4504	0.1498
TPI (msec)	6,939 [3,647–11,406]	5,962 [2,982–42,683]	4,200 [2,314–8,354]	>0.9999	0.0287	0.0404
MTT (msec)	20,992 [9,581–93,036]	12,303 [6,196–54,606]	5,541 [2,165–23,933]	>0.9999	0.0016	0.0003
Upslope	$1.46 \times 10^{-8}$ [7.23 × 10 <sup>-10</sup> –5.06 × 10 <sup>-8</sup> ]	$1.73 \times 10^{-8}$ [1.48 × 10 <sup>-10</sup> –7.25 × 10 <sup>-8</sup> ]	$3.64 \times 10^{-8}$ [3.23 × 10 <sup>-9</sup> –6.00 × 10 <sup>-7</sup> ]	>0.9999	0.1181	0.0406
Downslope	$1.27 \times 10^{-9}$ [6.42 × 10 <sup>-11</sup> –8.01 × 10 <sup>-9</sup> ]	$3.26 \times 10^{-9}$ [7.31 × 10 <sup>-11</sup> –9.18 × 10 <sup>-9</sup> ]	$1.25 \times 10^{-8}$ [1.01 × 10 <sup>-9</sup> –2.19 × 10 <sup>-7</sup> ]	>0.9999	0.0048	0.0018

Values are presented as median [range]. CA, cortical adenoma; CAC, cortical adenocarcinoma; PHEO, pheochromocytoma.

pattern, whereas CAC and PHEO exhibited a centripetal pattern. In addition, the vascularity of adrenal tumors in our study differed from that in a previous study [2]. In our study, the vascularity of CA was less than the vascularity of CAC and PHEO, whereas an opposite pattern was observed in a previous study [2]. The discrepancies were attributed to the differences in the contrast agent and qualitative analysis. Especially, the qualitative evaluation of CEUS depends strongly on the observers.

In human medicine, a CEUS enhancement pattern is not available for the differential diagnosis of adrenal mass lesions [8]. In contrast, CEUS using a TIC has been shown to identify malignant adrenal masses with a sensitivity of 100% and specificity of 67–82% based on an early arterial contrast-enhancement followed by a rapid decrease in enhancement [9, 10]. In our study, the qualitative assessment of the enhancement pattern could not differentiate between the various types of adrenal tumors, whereas quantitative assessments such as TPI, MTT, and downslope could distinguish between primary adrenal tumors of cortical and medullary origins in dogs, as in humans.

A previous study of triple-phase helical CT in canine adrenal tumors indicated that the characteristic CT findings of PHEO were a rapid wash-in and wash-out [32]. The characteristic CEUS findings of PHEO in our study were similar to the CT findings. However, the pre-contrast minimum CT values, washout of enhancement in the venous phase-delayed phase, and contrast homogeneity in the venous phase may represent the CT indicators for differentiation of CA and CAC [32]. In contrast, our study could not detect useful significant parameters from both qualitative and quantitative analyses of CEUS with respect to the differential diagnosis of canine adrenal cortical tumors. Further investigations of the differential diagnosis between CA and CAC based on CEUS findings are required. Currently, CEUS appears to be useful for differentiating the origins of canine adrenal tumors and as a convenient examination performed without anesthesia.

In canine CAC, the rupture of thin-walled vessels commonly causes areas of intratumoral hemorrhage [19]. This phenomenon is considered a cause for poor blood flow in the tumor. The histopathologic characteristics of CAC might include the highest rate of heterogeneous distribution of enhancement on CEUS. Histopathologically, a canine PHEO contains areas of telangiectasis in which islands of tumor cells are interspersed with distended, blood-filled vascular spaces and areas of hemorrhage [4]. The histopathologic findings of PHEO might produce the heterogeneous distribution of enhancement observed in the CEUS findings. In addition, the catecholamines synthesized in the PHEO could potentially induce tachycardia and hypertension, which might cause the rapid enhancement and decrement observed on CEUS. However, we did not observe any significant differences in the qualitative evaluation. Further investigations are needed to clarify the relationship between histopathological and CEUS findings.

Our study has certain limitations. First, due to the small sample size, our study did not include tumor types other than CA, CAC and PHEO and the CEUS finding in those tumors are unclear. Therefore, further investigations on adrenal CEUS are warranted after the collection of additional cases, including those involving other types of adrenal masses. Second, PHEO accounted for a large percentage (60%) of adrenal masses in our study, compared with previous studies [2, 24]. This difference might be attributable to the characteristics of our hospital, which is a referral hospital for advanced veterinary medical care. However, the

histopathological composition ratio of CA was relatively low, and therefore it might be difficult to differentiate between CA and CAC based on CEUS.

In conclusion, our study demonstrates that a quantitative assessment of CEUS data could distinguish the origins of primary canine adrenal tumors at a high level of specificity. Our findings suggest that CEUS is applicable for the differential diagnosis between primary adrenal tumors of cortical and medullary origins in dogs.

## REFERENCES

- Anderson, C. R., Birchard, S. J., Powers, B. E., Belandria, G. A., Kuntz, C. A. and Withrow, S. J. 2001. Surgical treatment of adrenocortical tumors: 21 cases (1990–1996). *J. Am. Anim. Hosp. Assoc.* **37**: 93–97. [[Medline](#)] [[CrossRef](#)]
- Bargellini, P., Orlandi, R., Dentini, A., Paloni, C., Rubini, G., Fonti, P., Diana, A., Peterson, M. E. and Boiti, C. 2016. Use of contrast-enhanced ultrasound in the differential diagnosis of adrenal tumors in dogs. *J. Am. Anim. Hosp. Assoc.* **52**: 132–143. [[Medline](#)] [[CrossRef](#)]
- Barrera, J. S., Bernard, F., Ehrhart, E. J., Withrow, S. J. and Monnet, E. 2013. Evaluation of risk factors for outcome associated with adrenal gland tumors with or without invasion of the caudal vena cava and treated via adrenalectomy in dogs: 86 cases (1993–2009). *J. Am. Vet. Med. Assoc.* **242**: 1715–1721. [[Medline](#)] [[CrossRef](#)]
- Barthez, P. Y., Marks, S. L., Woo, J., Feldman, E. C. and Matteucci, M. 1997. Pheochromocytoma in dogs: 61 cases (1984–1995). *J. Vet. Intern. Med.* **11**: 272–278. [[Medline](#)] [[CrossRef](#)]
- Behrend, E. N. 2015. Canine hyperadrenocorticism. pp. 377–451. *In: Canine and Feline Endocrinology*, 4th ed. (Feldman, E. C., Nelson, R. W., Reusch, C. E. and Scott-Moncrieff, J. C. eds.), Elsevier Saunders, St. Louis.
- Bertazzolo, W., Didier, M., Gelain, M. E., Rossi, S., Crippa, L., Avallone, G., Roccabianca, P., Bonfanti, U., Giori, L. and Fracassi, F. 2014. Accuracy of cytology in distinguishing adrenocortical tumors from pheochromocytoma in companion animals. *Vet. Clin. Pathol.* **43**: 453–459. [[Medline](#)] [[CrossRef](#)]
- Davis, M. K., Schochet, R. A. and Wrigley, R. 2012. Ultrasonographic identification of vascular invasion by adrenal tumors in dogs. *Vet. Radiol. Ultrasound* **53**: 442–445. [[Medline](#)] [[CrossRef](#)]
- Dietrich, C. F., Ignee, A., Barreiros, A. P., Schreiber-Dietrich, D., Sienz, M., Bojunga, J. and Braden, B. 2010. Contrast-enhanced ultrasound for imaging of adrenal masses. *Ultraschall Med.* **31**: 163–168. [[Medline](#)] [[CrossRef](#)]
- Friedrich-Rust, M., Glasemann, T., Polta, A., Eichler, K., Holzer, K., Kriener, S., Herrmann, E., Nierhoff, J., Bon, D., Bechstein, W. O., Vogl, T., Zeuzem, S. and Bojunga, J. 2011. Differentiation between benign and malignant adrenal mass using contrast-enhanced ultrasound. *Ultraschall Med.* **32**: 460–471. [[Medline](#)] [[CrossRef](#)]
- Friedrich-Rust, M., Schneider, G., Bohle, R. M., Herrmann, E., Sarrazin, C., Zeuzem, S. and Bojunga, J. 2008. Contrast-enhanced sonography of adrenal masses: differentiation of adenomas and nonadenomatous lesions. *AJR Am. J. Roentgenol.* **191**: 1852–1860. [[Medline](#)] [[CrossRef](#)]
- Gostelow, R., Bridger, N. and Syme, H. M. 2013. Plasma-free metanephrine and free normetanephrine measurement for the diagnosis of pheochromocytoma in dogs. *J. Vet. Intern. Med.* **27**: 83–90. [[Medline](#)] [[CrossRef](#)]
- Hatanaka, K., Kudo, M., Minami, Y. and Maekawa, K. 2008. Sonazoid-enhanced ultrasonography for diagnosis of hepatic malignancies: comparison with contrast-enhanced CT. *Oncology* **75** Suppl 1: 42–47. [[Medline](#)] [[CrossRef](#)]
- Hatanaka, K., Kudo, M., Minami, Y., Ueda, T., Tatsumi, C., Kitai, S., Takahashi, S., Inoue, T., Hagiwara, S., Chung, H., Ueshima, K. and Maekawa, K. 2008. Differential diagnosis of hepatic tumors: value of contrast-enhanced harmonic sonography using the newly developed contrast agent, Sonazoid. *Intervirology* **51** Suppl 1: 61–69. [[Medline](#)] [[CrossRef](#)]
- Herrera, M. A., Mehl, M. L., Kass, P. H., Pascoe, P. J., Feldman, E. C. and Nelson, R. W. 2008. Predictive factors and the effect of phenoxylbenzamine on outcome in dogs undergoing adrenalectomy for pheochromocytoma. *J. Vet. Intern. Med.* **22**: 1333–1339. [[Medline](#)] [[CrossRef](#)]
- Kyles, A. E., Feldman, E. C., De Cock, H. E., Kass, P. H., Mathews, K. G., Hardie, E. M., Nelson, R. W., Ilkiw, J. E. and Gregory, C. R. 2003. Surgical management of adrenal gland tumors with and without associated tumor thrombi in dogs: 40 cases (1994–2001). *J. Am. Vet. Med. Assoc.* **223**: 654–662. [[Medline](#)] [[CrossRef](#)]
- Lang, J. M., Schertel, E., Kennedy, S., Wilson, D., Barnhart, M. and Danielson, B. 2011. Elective and emergency surgical management of adrenal gland tumors: 60 cases (1999–2006). *J. Am. Anim. Hosp. Assoc.* **47**: 428–435. [[Medline](#)]
- Lunn, K. F. and Page, R. L. 2012. Tumors of the endocrine system. pp. 504–531. *In: Withrow and McEwen's Small Animal Clinical Oncology*, 5th ed. (Withrow, S. J., Vail, D. M. and Page, R. L. eds.), Elsevier Saunders, St. Louis.
- Massari, F., Nicoli, S., Romanelli, G., Buracco, P. and Zini, E. 2011. Adrenalectomy in dogs with adrenal gland tumors: 52 cases (2002–2008). *J. Am. Vet. Med. Assoc.* **239**: 216–221. [[Medline](#)]
- Meuten, D. J. 2002. Tumors of the adrenal gland. pp. 629–638. *In: Tumors in Domestic Animals*, 4th ed. (Capen, C. C. ed.), Blackwell Publishing, Ames.
- Nakamura, K., Lim, S. Y., Ochiai, K., Yamasaki, M., Ohta, H., Morishita, K., Takagi, S. and Takiguchi, M. 2015. Contrast-enhanced ultrasonographic findings in three dogs with pancreatic insulinoma. *Vet. Radiol. Ultrasound* **56**: 55–62. [[Medline](#)]
- Nakamura, K., Takagi, S., Sasaki, N., Bandula Kumara, W. R., Murakami, M., Ohta, H., Yamasaki, M. and Takiguchi, M. 2010. Contrast-enhanced ultrasonography for characterization of canine focal liver lesions. *Vet. Radiol. Ultrasound* **51**: 79–85. [[Medline](#)]
- Pagani, E., Tursi, M., Lorenzi, C., Tarducci, A., Bruno, B., Borgogno Mondino, E. C. and Zanatta, R. 2016. Ultrasonographic features of adrenal gland lesions in dogs can aid in diagnosis. *BMC Vet. Res.* **12**: 267–275. [[Medline](#)]
- Pey, P., Daminet, S., Smets, P. M., Duchateau, L., De Fornel-Thibaud, P., Rosenberg, D. and Saunders, J. C. 2013. Contrast-enhanced ultrasonographic evaluation of adrenal glands in dogs with pituitary-dependent hyperadrenocorticism. *Am. J. Vet. Res.* **74**: 417–425. [[Medline](#)]
- Pey, P., Rossi, F., Vignoli, M., Duchateau, L., Marescaux, L. and Saunders, J. H. 2014. Use of contrast-enhanced ultrasonography to characterize adrenal gland tumors in dogs. *Am. J. Vet. Res.* **75**: 886–892. [[Medline](#)]
- Pey, P., Vignoli, M., Haers, H., Duchateau, L., Rossi, F. and Saunders, J. H. 2011. Contrast-enhanced ultrasonography of the normal canine adrenal gland. *Vet. Radiol. Ultrasound* **52**: 560–567. [[Medline](#)]
- Salesov, E., Boretto, F. S., Sieber-Ruckstuhl, N. S., Rentsch, K. M., Riond, B., Hofmann-Lehmann, R., Kircher, P. R., Grouzmann, E. and Reusch, C. E. 2015. Urinary and plasma catecholamines and metanephrines in dogs with pheochromocytoma, hypercortisolism, nonadrenal disease and in healthy dogs. *J. Vet. Intern. Med.* **29**: 597–602. [[Medline](#)] [[CrossRef](#)]

27. Scavelli, T. D., Peterson, M. E. and Matthiesen, D. T. 1986. Results of surgical treatment for hyperadrenocorticism caused by adrenocortical neoplasia in the dog: 25 cases (1980–1984). *J. Am. Vet. Med. Assoc.* **189**: 1360–1364. [[Medline](#)]
28. Sumner, J. A., Lacordia, L., Rose, A. M., Woodward, A. P. and Carter, J. E. 2018. Clinical safety of percutaneous ultrasound-guided fine-needle aspiration of adrenal gland lesions in 19 dogs. *J. Small Anim. Pract.* **59**: 357–363. [[Medline](#)] [[CrossRef](#)]
29. Taeymans, O. and Penninck, D. 2011. Contrast enhanced sonographic assessment of feeding vessels as a discriminator between malignant vs. benign focal splenic lesions. *Vet. Radiol. Ultrasound* **52**: 457–461. [[Medline](#)] [[CrossRef](#)]
30. van Sluijs, F. J., Sjollem, B. E., Voorhout, G., van den Ingh, T. S. and Rijnberk, A. 1995. Results of adrenalectomy in 36 dogs with hyperadrenocorticism caused by adreno-cortical tumour. *Vet. Q.* **17**: 113–116. [[Medline](#)] [[CrossRef](#)]
31. Wills, T. B. and Haldorson, G. J. 2014. The adrenal gland. pp. 527–531. In: Cowell and Tyler's Diagnostic Cytology and Hematology of the Dog and Cat, 4th ed. (Valenciano A. C. and Cowell R. L. eds.), Elsevier Saunders, St. Louis.
32. Yoshida, O., Kutara, K., Seki, M., Ishigaki, K., Teshima, K., Ishikawa, C., Iida, G., Edamura, K., Kagawa, Y. and Asano, K. 2016. Preoperative differential diagnosis of canine adrenal tumors using triple-phase helical computed tomography. *Vet. Surg.* **45**: 427–435. [[Medline](#)] [[CrossRef](#)]